Journal of Nonlinear Mathematical Physics Volume 15, Supplement 3 (2008), 137–143 ARTICLE

Interchannel Soliton Collisions in Periodic Dispersion Maps in the Presence of Third Order Dispersion

Francisco J Díaz-Otero [a] and Pedro Chamorro-Posada [b]

[a] *Departamento de Teoría de la Señal y Comunicaciones, Universidad de Vigo, ETSI de Telecomunicación, Campus Universitario, 36200 Vigo, Spain*
E-mail: fjdiaz@com.uvigo.es

[b] *Departamento de Teoría de la Señal y Comunicaciones e Ingeniería Telemática, Universidad de Valladolid, ETSI Telecomunicación, Campus Miguel Delibes s/n, 47011 Valladolid, Spain*
E-mail: pedcha@tel.uva.es

Abstract

We study the effects of third order dispersion (TOD) on the collision of wavelength division multiplexed solitons in periodic dispersion maps. The analysis is based on a proposed ODE model obtained using the variational method which takes into account third order dispersion. The impact of TOD on the performance of high-speed optical transmission systems is discussed. The analysis presented focuses on the collision-induced frequency shifts of the pulses.

1 Introduction

The use of Dispersion Management (DM) techniques has permitted long-distance high-speed optical soliton based communication systems to become a practical reality [8]. This has been due mainly to a lessening of the penalties associated to certain degradation effects such as Gordon-Haus timing jitter, four-wave mixing (FWM) and collision induced frequency shifts and also to an improvement in the signal-to-noise ratio [10, 5].

Interchannel soliton collisions in wavelength division multiplexed (WDM) optical DM transmission systems induce shifts of their center frequencies which result in a crosstalk between channels and can severely impair system performance [1, 5, 10, 11]. The accurate modeling of WDM DM soliton transmission requires the inclusion of TOD, even though such effects have been routinely excluded in previous studies. Moreover, as the transmission requirements move to 40 Gb/s and 160 Gb/s for the synchronous optical network (SONET) and synchronous digital hierarchy (SDH), the impact of third order dispersion becomes quite appreciable even for a single channel transmission [6, 9, 7]. In this paper, we present an analysis of the impact of TOD effects in WDM DM soliton transmission systems by means of a new ODE model which takes into account TOD effects which has been obtained using the variational method [3]. To the authors knowledge, it's the first time that a TOD term is included in such a study.

2 Derivation of the ODE model using the variational method

The normalized complex envelope $u(Z,T)$ of an optical pulse in a periodic dispersion map evolves according to

$$j\frac{\partial u}{\partial Z}+\frac{1}{2}D(Z)\frac{\partial^2 u}{\partial T^2}+S(Z)\left|u\right|^2 u-j\delta(Z)\frac{\partial^3 u}{\partial T^3}=0, \tag{2.1}$$

where $\delta(Z)$ models the effect of TOD and $D(Z)$, T and Z represent the fiber dispersion, the retarded time and propagation distance, respectively. $S(Z)$ accounts for the effects of gain and loss. $D(Z)$ defines the dispersion map and is a periodic function of the propagation distance with alternating values D_+ and D_- in sections of fiber with lengths Z_+ and Z_- and average value D_{av}. $\Delta D = D_+ - |D_-|$ and $Z_0 = Z_+ + Z_-$ is the map period. TOD effects arise from $d^3\beta/d\omega^3$ where $\beta(\omega)$ is the mode propagation constant at frequency ω. The effects of the periodic loss and amplification in the system can be neglected in this analysis simply setting the term $S(Z)$ equal to 1. Such approach can be used in the approximate modeling of systems using novel Raman amplification schemes [4]. For the sake of simplicity, we assume a constant value for the TOD parameter δ.

In order to study the interchannel interactions between WDM solitons, we substitute $u(z,t) = u_1(z,t)+u_2(z,t)$ in (2.1), where u_l, $l=1,2$, are the waveforms of two pulses propagating in adjacent channels. We consider the frequency spacing between channels large enough in order to justify neglecting phase-sensitive terms and assume that interaction behavior is dictated by cross-phase modulation (XPM) effects alone. We obtain a system of two coupled generalized NLS equations

$$j\frac{\partial u_l}{\partial Z}+\frac{1}{2}D(Z)\frac{\partial^2 u_l}{\partial T^2}+S(Z)|u_l|^2u_l+2S(Z)|u_{3-l}|^2u_l-j\delta\frac{\partial^3 u_l}{\partial T^3}=0 \qquad l=(1,2). \tag{2.2}$$

The variational method [3] permits to reduce the full complexity of (2.2) to that of system of ODEs which capture the most relevant features of the evolving solutions in an approximate manner. The starting point is a Lagrangian density $\mathscr{L}(u_l,u_l^*)$ from which the condition [9]

$$\frac{\delta\mathscr{L}}{\delta u_l^*}\equiv\frac{\partial\mathscr{L}}{\partial u_l^*}-\frac{\partial}{\partial T}\frac{\partial\mathscr{L}}{u_{lT}^*}-\frac{\partial}{\partial Z}\frac{\partial\mathscr{L}}{\partial u_{lZ}^*}+\frac{\partial^2}{\partial^2 T}\frac{\partial\mathscr{L}}{\partial u_{lTT}^*}=0. \tag{2.3}$$

yields (2.2). The Lagrangian density

$$\mathscr{L}(u_l,u_l^*)=j\left(u_lu_{lZ}^*-u_l^*u_{lZ}\right)+D(Z)\left|u_{lT}\right|^2-S(Z)\left|u_l\right|^4-j\delta\left(u_{lTT}u_{lT}^*-u_{lTT}^*u_{lT}\right)-4S(Z)\left|u_{3-l}\right|^2\left|u_l\right|^2 \tag{2.4}$$

satisfies such condition.

Next, we assume that under strong dispersion management $|\Delta DZ_0|\gg 1$ [10] the pulse is well approximated by a Gaussian shape and use the ansatz

$$u_l\left(Z,T\right)=\sqrt{\frac{E_l}{\sqrt{\pi}}}\sqrt{p_l(Z)}\exp\left[-\frac{p_l(Z)^2}{2}\left(1-jC_l(Z)\right)\left(T-T_l(Z)\right)^2-j\omega_l\left(Z\right)\left(T-T_l(Z)\right)+j\theta_l\left(Z\right)\right] \tag{2.5}$$

where $E_l, p_l(Z), C_l(Z), \omega_l(Z), T_l(Z), \theta_l(Z)$ are the energy, inverse pulse width, linear chirp, center frequency, center position and phase of the pulse, respectively.

Substituting the ansatz in the Lagrangian density and integrating in the transverse coordinate T permits to obtain the Lagrangian for the reduced dynamical system

$$L = \frac{E_l}{2p_l^2}\left[p_l^2 C_l' + 2p_l p_l' C_l + D(Z)p_l^4(1+C_l^2) - 2\delta\omega_l p_l^4(1+C_l^2) - 4\delta\omega_l C_l^2 p_l^4\right]$$
$$+E_l\left[2\omega_l T_l' + 2\theta_l' + D(Z)\omega_l^2 - 2\delta\omega_l p_l^2 - 2\delta\omega_l^3\right] - S(Z)\frac{E_l^2 p_l}{\sqrt{2\pi}}$$
$$-4S(Z)\frac{E_l E_{3-l} p_l p_{3-l}}{\sqrt{\pi}\sqrt{p_l^2 + p_{3-l}^2}}\exp(-P^2\Delta T_l^2/2) \tag{2.6}$$

where the primes stand for the derivatives with respect to Z and

$$P = \frac{\sqrt{2}p_l p_{3-l}}{\sqrt{p_l^2 + p_{3-l}^2}}. \tag{2.7}$$

Finally, taking the variation with respect to each of the pulse parameters p_l, C_l, ω_l, T_l, we obtain the equations of motion

$$\frac{dp_l}{dZ} = -C_l p_l^3\left(D - 6\delta\omega_l\right) \tag{2.8}$$
$$\frac{dC_l}{dZ} = \left(1+C_l^2\right)\left(D - 6\delta\omega_l\right)p_l^2 - \frac{p_l S(Z)}{\sqrt{2\pi}}\left(E_l + 2E_{3-l}p_l^3\left(1-\tau_l^2\right)\exp\left(-\frac{\tau_l^2}{2}\right)\right) \tag{2.9}$$
$$\frac{dT_l}{dZ} = -D\omega_l + 3\delta\omega_l^2 + \frac{3}{2}\delta\left(1+C_l^2\right)p_l^2 \tag{2.10}$$
$$\frac{d\omega_l}{dZ} = \frac{2E_{3-l}S(Z)}{\sqrt{2\pi}}\tau_l P^2\exp\left(-\frac{\tau_l^2}{2}\right) \tag{2.11}$$

where

$$\tau_l = P\Delta T_l, \tag{2.12}$$
$$\Delta T_l = T_l - T_{3-l} \tag{2.13}$$

and

$$S(Z) = g_0\exp(-2\Gamma Z) \tag{2.14a}$$
$$g_0 = \frac{2\Gamma Z_a}{1-\exp(-2\Gamma Z_a)}. \tag{2.14b}$$

Figure 1 shows the evolution of the parameters describing the pulse in the $\omega_1 = -17.75$ channel during the collision with another pulse simultaneously propagating in the same fiber link in the $\omega_2 = 17.75$ channel. Both the results obtained from the integration of the ODE system (2.8)-(2.11) and the parameters estimated from the results of the numerical integration of the PDE (2.1) using the split-step Fourier method [2] are displayed and excellent agreement is found between the two sets of values. The map parameters used in the simulation are $\Delta D = 20$, $\delta = 5e^{-4}$ and $D_{av} = 1$.

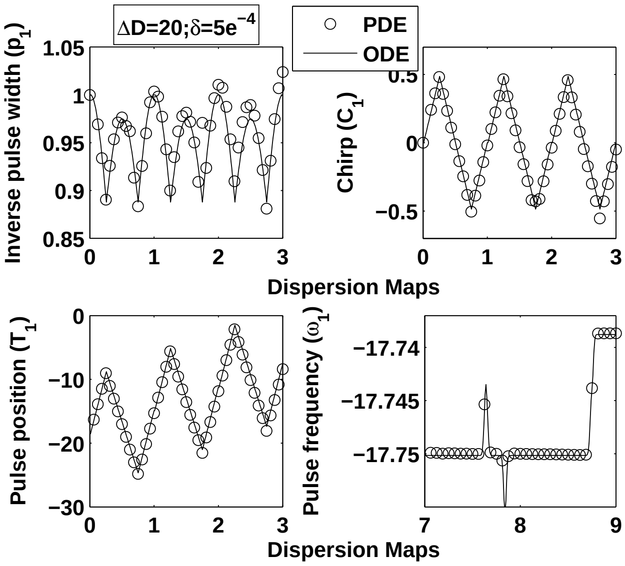

Figure 1. Evolution of the pulse parameters p_1, C_1, T_1 and ω_1 as obtained from the ODEs (2.8)-(2.11) and estimated from the results obtained of the numerical solution of the PDE (2.1).The lower right panel shows an expanded view of the collision area.

3 Results and discussion

When compared to the corresponding variational equations in the absence of TOD [10], the evolution equations derived in the previous section reveal a correction of the effective dispersion as $D_{eff} = D - 6\delta\omega$. This also results in an effective modification of the map parameters for each channel. In fact, for sufficiently large values of ω, one works in a regime where the periodic DM solutions no longer exist.

Figure 2 illustrates how the properties of a single channel stationary pulse vary with δ due to the changes in the effective dispersion. For the analysis, we set $E_2 = 0$ in Eqs. (2.8)-(2.11) and keep only the results of the parameters for the $l = 1$ pulse. As for all the simulations in this section, we consider $p(0) = 1$ pulses launched in the chirp-free point $C(0) = 0$ at the midpoint of the anomalous dispersion segment of a normalized map with $Z_+ = Z_- = 0.5$ and $D_{av} = 1$. In the absence of interactions, we find from Eq. (2.11) that $\omega_l(Z) = \omega_l(0)$. The left panel shows the pulse energy E required for the pulse to exhibit a periodic evolution in the map as a function of the dispersion difference ΔD for both the $\omega_1 = -17.75$ (top) and the $\omega_1 = 17.75$ (bottom) channels. When $\delta > 0$, the change in effective dispersion results in an increase of the required input energy E for the $\omega < 0$ channel and a decrease of E for the $\omega > 0$ channel. The right panel shows the dynamical evolution of the system in the (p,C) plane for the $\omega_1 = -17.75$ case. For each value of δ, as the energy required to maintain the periodicity of the solution at the $(p,C) = (1,0)$ point becomes greater, the size of the trajectory in the phase plane increases. The reciprocal situation is found for the $\omega_1 = 17.75$ pulse: the trajectory in the phase plane contracts as the required input energy E decreases. For $\delta < 0$ the situation is reversed and the required energy is greater for $\omega > 0$.

We now consider the simultaneous propagation of two pulses with $\omega_1(0) = -\omega_2(0) = -17.75$ and initial positions $T_1(0) = -T_2(0) = -22.2$. The group velocity dispersion will drive the motion of the pulses with non-vanishing frequency shift in the normalized framework as given by Eq.

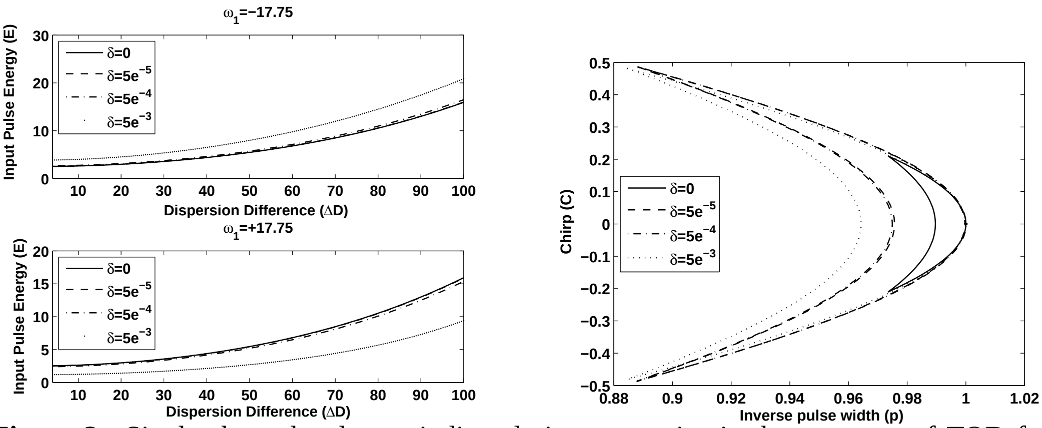

Figure 2. Single-channel pulse periodic solution properties in the presence of TOD for different frequency channels. Left panel: Input pulse energy required for stable pulse propagation for different values of δ for $\omega_1 = -17.75$ (top) and $\omega_1 = 17.75$ (bottom). Right panel: Phase-plane dynamics for lossless DM transmission in the $\omega_1 = -17.75$ channel for different values of the TOD parameter δ.

(2.10). If we neglect the last term in (2.11), which is $O(\delta)$, the pulse trajectories are approximately described by

$$V_l \simeq -D\omega_l + 3\delta\omega_l^2, \tag{3.1}$$

where V_l is the *transverse velocity* of the $l-$th pulse and it is related with the inverse of its group velocity.

As a pulse propagates in the dispersion map, it describes a zigzag trajectory where the direction of the displacement alternates following the changes in the sign of $D(Z)$ (see Figure 1). When V_l has a different average value for $l = 1$ and $l = 2$ two pulses with a large initial separation are brought together and collide. Soliton collisions in WDM DM transmission lines cause residual frequency shifts which, in turn, produce timing jitter at the receiver [10]. This effect can severely degrade the system performance.

In order to analyze qualitatively how TOD affects the collisions, we use the approximate result given in Eq. (3.1) and assume $\omega_1 \simeq -\omega \simeq -\omega_2$, with $\omega > 0$. First, we find that the symmetry in the movement of the two solitons is lost, since $|V_1| \neq |V_2|$. Nevertheless, the net relative transverse velocity for any value of δ is $V_{1,2} = V_1 - V_2 \simeq -2D\omega$ which is approximately the same as the value found for $\delta = 0$. So, the asymmetry of the interaction process does not affect the strength of the nonlinear interaction due to XPM.

Figure 3.a displays the frequency shift for the $l = 1$ channel. One finds that the main effect of TOD is to decrease the residual frequency shift for this channel, while maintaining both the characteristic oscillatory profile along the dispersion difference axis and the positions of the local minima for the frequency shift at $\Delta D = 4n + 6$. In the inset, we observe a 6 per cent reduction of the residual frequency shift for $\delta = 5e^{-4}$ and a 47 per cent for $\delta = 5e^{-3}$ at $\Delta D = 12$. Figure 3.b shows the corresponding results for the $l = 2$ channel and we observe the converse effect: an increase of the residual frequency shift. A change in the sign of δ produces a swap in the roles of the two channels.

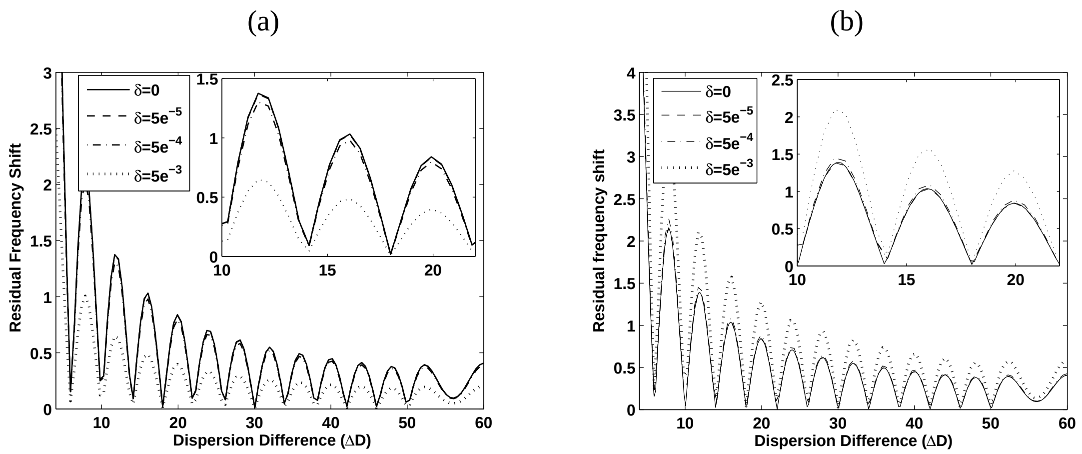

Figure 3. Residual freq shift vs. dispersion difference in a periodic DM line with parameters as described in the text for $\omega_1 = 17.75$ (a) and $\omega_2 = -17.75$ (b).

The results shown in Figure 3 can be explained in terms of the values of the required input energy for the two channels. TOD produces a variation of the effective dispersion, so, for fixed $\delta > 0$, as ω increases, larger values of E_1 and smaller values of are E_2 are required for the input pulses. This means that the $l = 2$ channel experiences stronger nonlinear interaction due to XPM, as described in Eq. (2.11), whereas the impairment is smaller for the $l = 1$ channel. The results can be extrapolated to a larger number of channels: each channel suffers of stronger nonlinear effects due to those neighboring channels with smaller carrier frequencies than from those with larger frequencies. This sets a privileged situation for the channel at the lower end of the frequency multiplex. The degradation due to nonlinear interaction should worsen as the position in the frequency multiplex moves to higher frequencies. If the sign of δ is reversed, the whole picture is reversed and the "preferred" channel is that with the smaller frequency.

Acknowledgments. This work has been funded by MEC and FEDER, project number TEC2007-67429-C01 and TEC2007-67429-C02.

References

[1] ABLOWITZ M, BIONDINI G, BISWAS A, DOCHERTY A, HIROOKA T and CHAKRAVARTY S, Collision-induced timing shifts in dispersion-managed soliton systems, *Opt. Lett.* **27** (2002), 318-320.

[2] AGRAWAL G P, Nonlinear fiber optics, 3rd ed., San Diego: Academic Press, 2001.

[3] ANDERSON D, Variational approach to nonlinear pulse propagation in optical fibers, *Phys. Rev. A* **27** (1983), 3135.

[4] ANIA-CASTAÑON J D, Quasi-lossless transmission using second-order Raman amplification and fiber Bragg gratings, *Opt. Exp.* **12** (2004), 4372.

[5] HIROOKA T and HASEGAWA A, Chirped soliton interaction in strongly dispersion-managed wavelength-division-multiplexed-systems, *Opt. Lett.* **23** (1998), 768-770.

[6] LAKOBA T and AGRAWAL G, Effects of third-order dispersion on dispersion-managed solitons, *J. Opt. Soc. Am. B* **16** (1999), 1332.

[7] MISHRA M and KONAR S, High bit rate dense dispersion managed optical communication systems iwth distributed amplification, *PIER* **78** (2008), 301.

[8] MOLLENAUER L F and GORDON J P, Solitons in optical fibers: fundamentals and applications, Amsterdam/Boston : Elsevier/Academic Press, 2006.

[9] MOOKHERJEA S and YARIV A, Hamiltonian dynamics of breathers with third-order dispersion, *J. Opt. Soc. Am. B* **18** (2001), 1150.

[10] SUGAHARA H, KATO H, INOUE T, MARUTA A and KODAMA Y, Optimal dispersion management for a wavelength division multiplexed optical soliton transmission system, *Journal of Lightwave Tech.* **17** (1999), 1547–1559.

[11] SUGAHARA H, KATO H and KODAMA Y, Maximum reduction of collision induced frequency shift in soliton-WDM systems with dispersion compensation, *Elect. Lett.* **33** (1997), 1065-1066.